Nuclear Engineering and Technology 49 (2017) 395–403

Available online at ScienceDirect

Nuclear Engineering and Technology

journal homepage: www.elsevier.com/locate/net

Original Article

An Evaluation Method for Tornado Missile Strike Probability with Stochastic Correlation

Yuzuru Eguchi[*], *Takahiro Murakami*, *Hiromaru Hirakuchi*, *Soichiro Sugimoto*, *and Yasuo Hattori*

Nuclear Risk Research Center (External Natural Event Research Team), Central Research Institute of Electric Power Industry, Abiko 1646, Abiko-shi, Chiba-ken 270-1194, Japan

ARTICLE INFO

Article history:
Received 5 December 2016
Accepted 11 December 2016
Available online 6 January 2017

Keywords:
Correlation
Missile
Strike Probability
Tornado
Wind Speed

ABSTRACT

An efficient evaluation method for the probability of a tornado missile strike without using the Monte Carlo method is proposed in this paper. A major part of the proposed probability evaluation is based on numerical results computed using an in-house code, Tornado-borne missile analysis code, which enables us to evaluate the liftoff and flight behaviors of unconstrained objects on the ground driven by a tornado. Using the Tornado-borne missile analysis code, we can obtain a stochastic correlation between local wind speed and flight distance of each object, and this stochastic correlation is used to evaluate the conditional strike probability, $Q_V(r)$, of a missile located at position r, where the local wind speed is V. In contrast, the annual exceedance probability of local wind speed, which can be computed using a tornado hazard analysis code, is used to derive the probability density function, $p(V)$. Then, we finally obtain the annual probability of tornado missile strike on a structure with the convolutional integration of product of $Q_V(r)$ and $p(V)$ over V. The evaluation method is applied to a simple problem to qualitatively confirm the validity, and to quantitatively verify the results for two extreme cases in which an object is located just in the vicinity of or far away from the structure.

1. Introduction

Tornadoes can produce airborne missiles because of their high-speed wind, and missile impact on structures, systems, and components of a nuclear power plant could lead to physical and functional damage with possible deviation from normal plant conditions. To understand such risk induced by tornado missiles, we need to evaluate not only the degree of potential damage incurred but also the probability of the occurrence. In the USA, probabilistic evaluation of tornado missile hazard and fragility was intensively studied in the 1980s. In particular, the Electric Power Research Institute developed a probabilistic computer code for tornado missile risk analysis, TORMIS, to compute the damage probability and its uncertainty range [1–3]. In recent years, Tornado Missile Strike Calculator has been developed by Westinghouse Electric Company (Windsor, CT, USA) [4], which has demonstrated that Tornado Missile Strike Calculator is capable of yielding

* *Corresponding author.*
E-mail address: eguchi@criepi.denken.or.jp (Y. Eguchi).
http://dx.doi.org/10.1016/j.net.2016.12.007

reasonable results comparable to those of TORMIS. In these tools, the probability of a missile strike is computed using the Monte Carlo method with the running of an enormous number of simulation cases.

The objective of this study is to formulate an efficient evaluation method for the probability of a tornado missile strike without using the Monte Carlo method. In this study, the tornado missile liftoff and flight behaviors are computed by our in-house software, named Tornado-borne missile analysis code (TONBOS) [5,6], which enables us to reasonably compute dynamic behaviors for unconstrained objects placed on the ground, such as automobiles. The numerical results are used to obtain a stochastic correlation between the local wind speed at 10 m above ground level (AGL), V, and the flight distance, L; with these pieces of information, the conditional strike probability can be efficiently computed. In contrast, the annual exceedance probability of local wind speed, computed with a tornado hazard analysis code, is used to obtain the probability density function of the local wind speed. Then, the annual probability of tornado missile strike on a structure is computed using the convolutional integration of both ingredients [7]. In the following section, we will fully explain the evaluation scheme for annual missile strike probability. As a numerical example, the method is applied to automobiles on the ground to compute the annual strike probability on a cylindrical structure, as explained in Section 3. We shall discuss the validity of the results and the effects of tornado pressure distribution on the flight behavior in Section 4 and draw conclusions in Section 5.

2. Materials and methods

2.1. Overall framework

Fig. 1 shows the overall framework of the proposed evaluation method. First, a correlation between local wind speed, V, and flight distance, L, is obtained from the numerical results of TONBOS and is used to compute the conditional probability density function, $S_V(L)$, with respect to the flight distance under a specific local wind speed condition. Then, conditional strike probability, $Q_V(\mathbf{r})$, can be obtained via convolutional integration of the product of $S_V(L)$ and $q(\mathbf{r},L)$ over L, where $q(\mathbf{r},L)$ is the strike probability of an object (possible missile) at position $\mathbf{r}$, whose flight distance is L. By contrast, the annual exceedance probability of local wind speed, $H(V)$, computed with a tornado hazard analysis code, e.g., Tornado Wind Speed Hazard Model for Limited Area (TOWLA) [8], is used to obtain the probability density function, $p(V)$, by differentiation of $H(V)$ with respect to V. Then, we can finally obtain the annual probability of tornado missile strike on a structure, $P_h(\mathbf{r})$, with the convolutional integration of the product of $Q_V(\mathbf{r})$ and $p(V)$ over V.

The basic equations used in TONBOS for the missile liftoff and for the flight model are explained in Subsection 2.2, whereas those for the tornado wind field model are provided in Subsection 2.3. In Subsection 2.4, it is explained how we can obtain the conditional probability density function, $S_V(L)$, that represents the stochastic correlation between local wind speed V and flight distance L. In Subsection 2.5, we discuss the evaluation scheme for annual missile strike probability, particularly how the tornado hazard curve, $H(V)$, is combined with the conditional strike probability.

2.2. Missile liftoff and flight model of TONBOS

A user of TONBOS can select either the Fujita model (DBT-77) [9] or the Rankine vortex model [10,11] as a tornado wind field model, while motion of objects in flight is modeled with 3 degrees-of-freedom translational equations in which aerodynamic drag force and gravity are taken into account [10,11]. The unique feature of TONBOS is that objects are assumed to be subject to lift force near the ground; this force is generated by asymmetric air flow around objects because of the ground effect.

2.2.1. Liftoff model

Objects on and near the ground are assumed to be subject to lift force generated by asymmetric air flow because of the

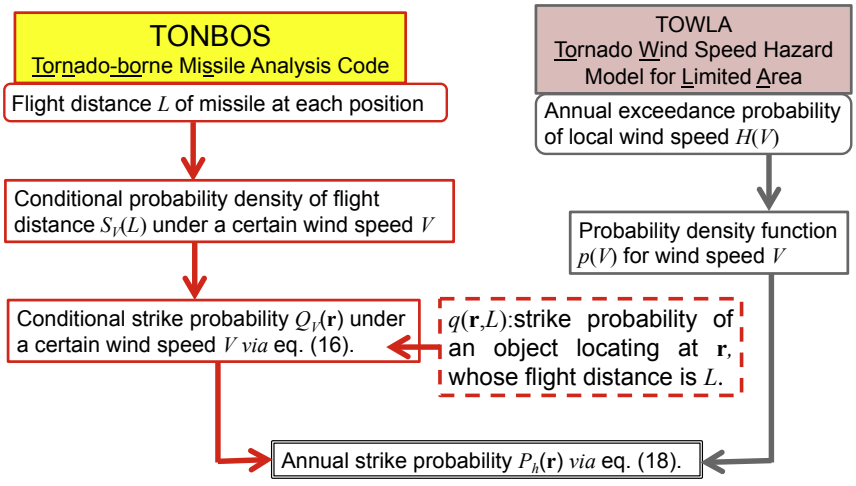

Fig. 1 – Computational flow of annual strike probability.

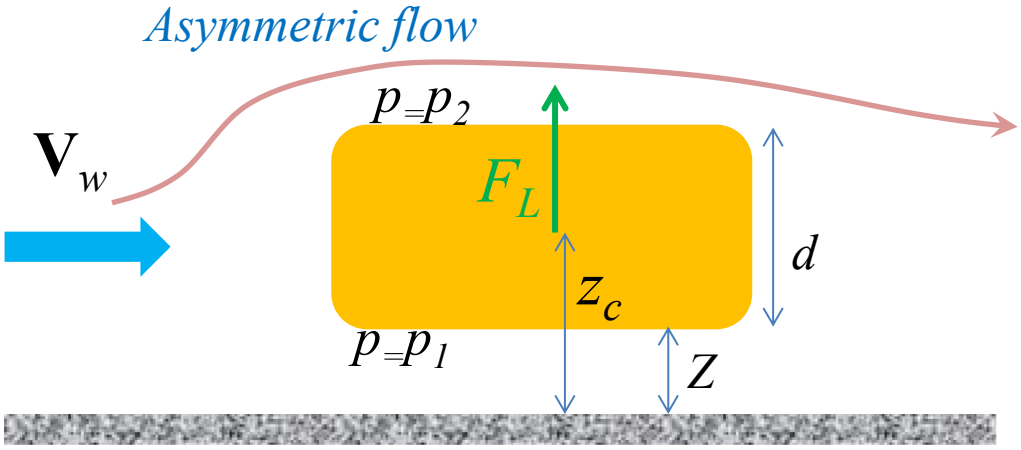

Fig. 2 – Flow pattern around object on/near the ground.

ground effect, as shown in Fig. 2. This lift force, F_L, is expressed by a lift coefficient, $C_L(z_c)$, in combination with the relative wind velocity, $\mathbf{V}_w - \mathbf{V}_M$, and the projection area, a, as follows:

$$F_L = \frac{1}{2}\rho C_L(z_c) a |\mathbf{V}_w - \mathbf{V}_M|^2_{x,y}, \quad (1)$$

where $\mathbf{V}_w$ and $\mathbf{V}_M$ are the wind velocity vector and the missile velocity vector, respectively; z_c is the elevation of the object center from ground level; ρ is the air density; and $|\mathbf{V}_w - \mathbf{V}_M|_{x,y}$ denotes the magnitude of the horizontal component of the relative velocity vector, $\mathbf{V}_w - \mathbf{V}_M$. To maintain conservatism and to increase practicability, the authors proposed the following model instead of Eq. (1) in TONBOS [5,6].

$$F_L = \frac{1}{2}\rho C_D A f(Z/d) |\mathbf{V}_w - \mathbf{V}_M|^2_{x,y}, \quad (2)$$

where $C_D A$ and $f(Z/d)$ are defined as follows:

$$C_D A = \frac{C_{D_x} A_x + C_{D_y} A_y + C_{D_z} A_z}{3} \quad (3)$$

$$f(Z/d) = \begin{cases} \dfrac{1-(Z/3d)}{1+(Z/d)} & (0 \le Z \le 3d) \\ 0 & (3d < Z) \end{cases}, \quad (4)$$

where C_{D_i} and A_i are, respectively, a drag coefficient and a projection area for i-direction flow, and Z is the gap between an object and the ground, i.e., $Z = z_c - d/2$, where d is object height. The conservatism of Eq. (2) can be justified with various experimental data described in relevant works in the literature [12–17].

2.2.2. *Flight model*

In TONBOS, the 3 degrees-of-freedom dynamic equation is used for simulations of missile flight motion, as originally proposed by Simiu and Cordes [10] as well as Simiu and Scanlan [11]. The schematic image of the dynamic motion of a missile is depicted in Fig. 3; the basic equation can be written in the following form, taking the ground effect into account.

$$\frac{d\mathbf{V}_M}{dt} = \frac{1}{2}\rho \frac{C_D A}{m} |\mathbf{V}_w - \mathbf{V}_M| (\mathbf{V}_w - \mathbf{V}_M) - (g - L)\mathbf{k}, \quad (5)$$

where t is the time, m is the mass of the missile, g is the gravitational acceleration, and $\mathbf{k}$ is a unit vector in the z direction. The lift acceleration due to the ground effect, L, is defined as follows:

$$L = \frac{F_L}{m} = \frac{1}{2}\rho \frac{C_D A}{m} f(Z/d) |\mathbf{V}_w - \mathbf{V}_M|^2_{x,y}, \quad (6)$$

where $C_D A/m$ is the flight parameter.

2.3. *Tornado wind field model*

The typical wind velocity vectors of the Fujita model [9] are shown on a tornado center cross section in Fig. 4. It can be seen that the central region of a tornado is divided into an

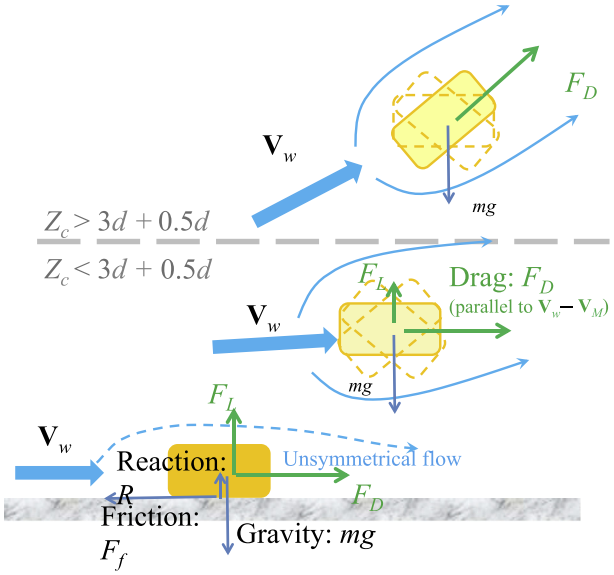

Fig. 3 – Schematic image of the dynamic motion of a missile modeled in TONBOS. TONBOS, Tornado-borne missile analysis code.

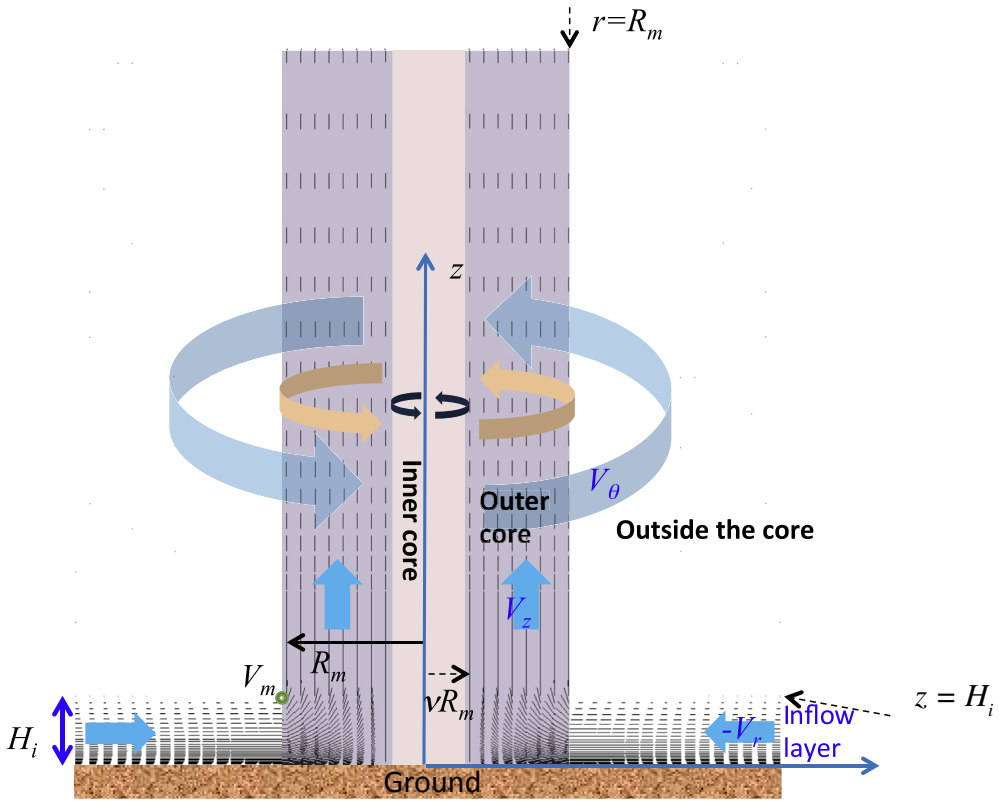

Fig. 4 – Cross-sectional view of wind field of Fujita model.

inner core and an outer core, whose maximum radii are denoted by R_i and R_m, respectively; these two values are related by the following formula, proposed by Fujita [9].

$$R_i = \nu R_m \tag{7}$$

$$\nu = 0.9 - 0.7\exp(-0.005R_m), \tag{8}$$

where R_m is expressed in meters. The Fujita model also postulates a boundary layer near the ground, called the inflow layer, whose height is denoted by H_i and is related with the following empirical formulae.

$$H_i = \eta R_m \tag{9}$$

$$\eta = 0.55(1-\nu^2) \tag{10}$$

In the following, all the velocity components of the Fujita model are written as functions of the nondimensional radius $\underline{r}$ ($= r/R_m$) and the nondimensional axial coordinate $\underline{z}$ ($= z/H_i$). The tangential wind speed V_θ is expressed as follows [9]:

$$V_\theta(r,z) = \min\left(\underline{r}, \underline{r}^{-1}\right) \times \min\left(\underline{z}^{k_0},\ \exp\{-k(\underline{z}-1)\}\right) \times V_m, \tag{11}$$

where V_m is the maximum horizontal velocity of vortical flow excepting translational velocity; this value of V_m is equal to the maximum tangential velocity in the Fujita model.

For constants k_0 and k, we set $k_0 = 1/6$ and $k = 0.03$ as recommended in the Fujita model [9]. The radial component, V_r, which has a positive value for the outward direction, is derived from the continuity law of fluids, as shown below.

$$V_r(r,z) = \begin{cases} 0 & (\underline{r} \le \nu) \\ \dfrac{V_\theta \tan\alpha_0}{1-\nu^2}\left(1-\dfrac{\nu^2}{\underline{r}^2}\right) & (\nu < \underline{r} < 1) \\ V_\theta \tan\alpha_0 & (\underline{r} \ge 1) \end{cases} \tag{12a}$$

$$\tan\alpha_0 = \begin{cases} -A\left(1-\underline{z}^{1.5}\right) & (\underline{z} < 1) \\ B\{1-\exp(-k(\underline{z}-1))\} & (\underline{z} \ge 1) \end{cases} \tag{12b}$$

The upward wind speed, V_z, is defined by Eq. (13); this value exists only in the outer core region and is independent of the radial and azimuthal positions in the region.

$$V_z(z) = \begin{cases} \dfrac{3}{28}\dfrac{\eta V_m}{1-\nu^2}A\left(16\underline{z}^{\frac{7}{6}} - 7\underline{z}^{\frac{8}{3}}\right) & (\underline{z} < 1) \\ \dfrac{\eta V_m B\exp(-k(\underline{z}-1))}{k(1-\nu^2)}\{2-\exp(-k(\underline{z}-1))\} & (\underline{z} \ge 1) \end{cases}, \tag{13}$$

where A and B are constants; we use a recommended value of 0.75 for A, whereas the constant B is given by $B = 3kA/(k_0+1)(k_0+2.5)$, so that the velocities abide by the continuity constraint.

Equation (14) describes the wind velocity, $\mathbf{V}_w$, in Cartesian coordinates by assuming that a tornado moves translationally toward the $+x$ direction with a constant speed, V_{tr}.

$$\mathbf{V}_w = \begin{pmatrix} \cos\theta & -\sin\theta & 0 \\ \sin\theta & \cos\theta & 0 \\ 0 & 0 & 1 \end{pmatrix} \begin{pmatrix} V_r \\ V_\theta \\ V_z \end{pmatrix} + \begin{pmatrix} V_{tr} \\ 0 \\ 0 \end{pmatrix}, \quad (14)$$

where θ is the azimuthal angle shown in Fig. 5 and the radial distance at (x, y, z), r, is defined by $r^2 = (x - V_{tr}T)^2 + y^2$ at $t = T$, assuming that the center of the tornado is initially located at the origin ($t = 0$).

2.4. Stochastic correlation between wind speed and flight distance

Assuming the wind field of a translating tornado defined by the Fujita model, local wind speed, V, which is defined as the largest horizontal wind speed at 10 m AGL experienced during a whole tornado action, can be calculated at an arbitrary point (x, y, 10) using Eq. (14). By contrast, the flight distance L of objects initially placed around a tornado path, such as that shown in Fig. 6, can be computed using TONBOS. Flight distance L is dependent on the location of each point relative to the tornado position and the translating direction. In particular, objects around the origin tend to fly for long distances, because a tornado is assumed to suddenly appear at the origin at $t = 0$, imposing high wind on objects around the origin. By contrast, objects initially placed in the downwind side ($+x$ region) tend to fly for short distances, because the objects will be picked up by wind of lower speed, flying at rather low altitudes and hitting the ground quickly. To be conservative, in our method the flight distance computed is represented by the maximum value at the upwind side (or $-x$ direction).

Based on these numerical results, we are able to compute the conditional probability density function, $S_V(L)$, with respect to the flight distance under a specific local wind speed condition, for which the following mathematical restriction should be satisfied.

$$\int_0^\infty s_V(L)dL = 1 \quad (15)$$

It should be noted that probability density function $S_V(L)$ can be expressed as a delta function $\delta(L)$ for $V < V_c$, where V_c is the minimum local wind speed at 10 m AGL required for liftoff. In other words, objects will not be lifted and will not be transported by tornado at all (i.e., $L = 0$) if the local wind speed is below the critical local wind speed, V_c.

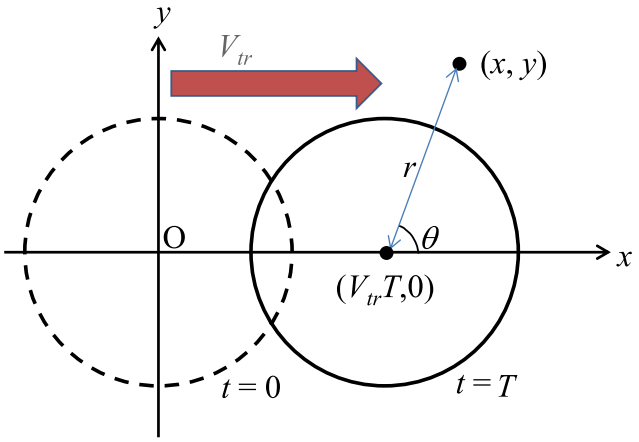

Fig. 5 – Translational motion of tornado.

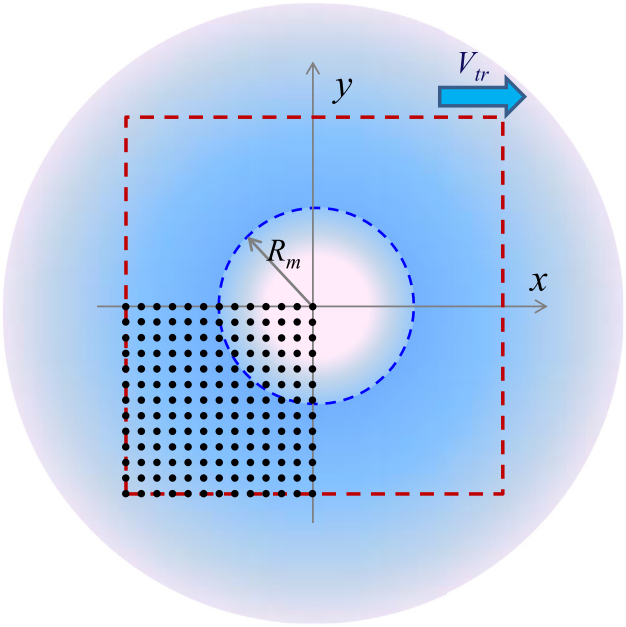

Fig. 6 – Arrayed arrangement of objects around a tornado.

2.5. Conditional strike probability and annual strike probability

Whether an object would strike a target should generally depend on the flight path of the object, including such factors as the flight distance, height, and direction relative to the target. In our method, we presume that tornadoes that attack a site do not have any preferential direction along their paths, which means that the probability of missile flight direction is uniform. A further presumption is that the strike probability, q, of an object placed at position r relative to the target can be approximately expressed only by the flight distance, L, such as q(r,L). In such a case, the conditional strike probability under a specific local wind speed condition, $Q_V(r)$, can be obtained by the integration of product of $S_V(L)$ and q(r,L) over L, as shown in Eq. (16).

$$Q_V(\mathbf{r}) = \int_0^\infty q(\mathbf{r}, L)S_V(L)dL \quad (16)$$

By contrast, the annual exceedance probability of local wind speed H(V) can be computed using a tornado hazard analysis code (e.g., TOWLA) [8]. The probability density function, p(V), for local wind speed V is obtained as follows through the differentiation of H(V) with respect to V, with a negative sign.

$$p(V) = -\frac{dH(V)}{dV} \quad (17)$$

Then, the annual probability of tornado missile strike on a structure, $P_h(\mathbf{r})$, is computed with the convolutional integration of the product of $Q_V(\mathbf{r})$ and p(V) over V, as shown below:

$$P_h(\mathbf{r}) = \int_0^{V_{m,l}} p(V)Q_V(\mathbf{r})dV = \int_{V_c}^{V_{m,l}} p(V)Q_V(\mathbf{r})dV, \quad (18)$$

where $V_{m,l}$ is the maximum value of the local wind speed.

3. Results

As a numerical example, we shall compute the annual strike probability of an automobile on a tall cylindrical structure. Assuming that the mass of an automobile is 1,140 kg, and the dimensions are 4.4 m (length) × 1.7 m (width) × 1.5 m (height), the flight parameter, C_DA/m, of the automobile is calculated as 0.0097 m^2/kg via Eq. (3). The automobile is assumed to be at radius r from the center of the tall cylindrical structure, whose radius is 20 m ($R_t = 20$ m), as shown in Fig. 7. As for the tornado condition, a maximum wind speed of 92 m/s ($V_m = 78$ m/s, $V_{tr} = 14$ m/s) and a core radius, R_m, of 30 m are assumed here.

Local wind speeds at 10 m AGL were computed using the Fujita model wind field at 58,081 (241 × 241) points within a 120 m × 120 m square region; the spatial distribution is shown in Fig. 8. It can be seen that a higher local wind speed exists around $y = -R_m$, because the tornado is assumed to rotate counterclockwise and translates in the $+x$ direction. Meanwhile, flight distances were computed with TONBOS for automobiles located at the same points within the 120 m × 120 m square region. As shown in Fig. 9, flight distance is dependent on the relative location around the origin, but independent of the x coordinate at the downwind side ($+x$ region) because, to assure conservative evaluation, the flight distance was replaced by the maximum value at the upwind side, as explained in Subsection 2.4. A phase plot of the local wind speed, V, and the flight distance, L, is shown in Fig. 10, where

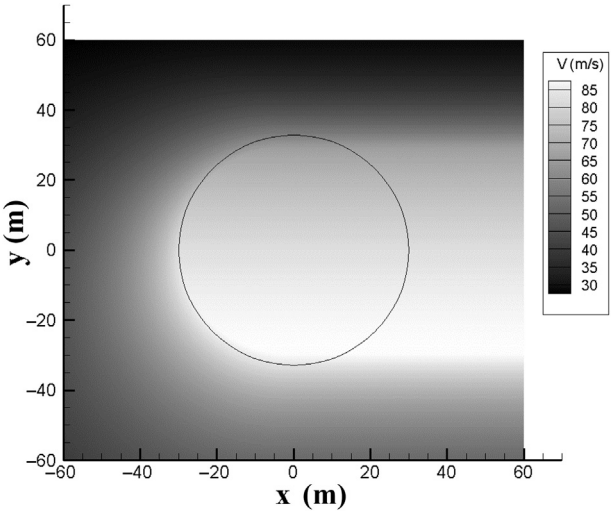

Fig. 8 – Distribution of local wind speed, V.

we can see that the critical local wind speed (V_c) is about 45 m/s, the maximum value of the local wind speed (V_m) is about 90 m/s, and the maximum value of the flight distance (L_m) is about 85 m.

The probability density function, $S_V(L)$, corresponding to the data in Fig. 10, is shown in Fig. 11. High values of $S_V(L)$ can be seen near the right-hand side end (boundary between zero and nonzero distribution) in this figure. This is because the flight distance in the downwind region was replaced by the maximum value at the upwind side, as mentioned above.

Considering the geometrical condition of the target structure relative to the automobile, as shown in Fig. 12, the strike probability, $q(\mathbf{r},L)$, of an automobile placed at radius $r = |\mathbf{r}|$ from

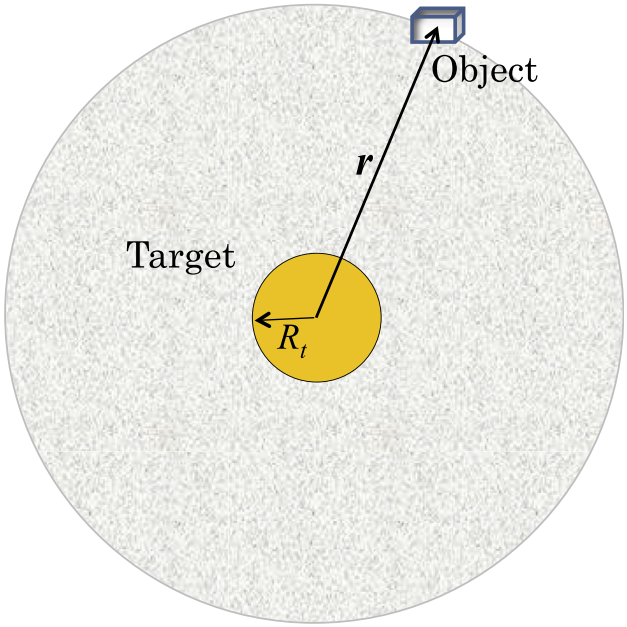

Fig. 7 – Arrangement of object (automobile) and cylindrical target.

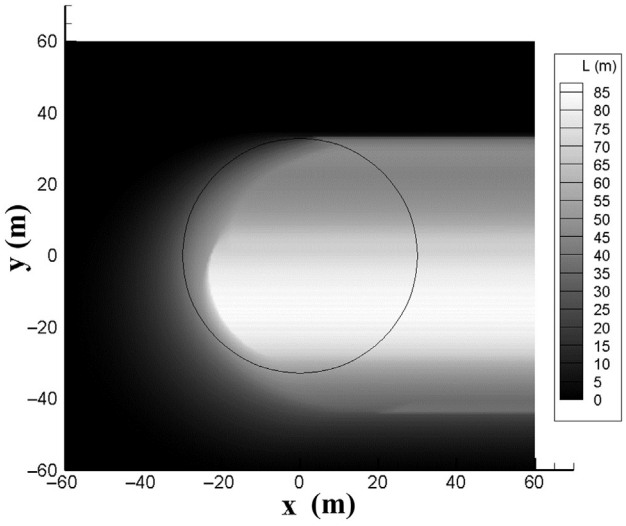

Fig. 9 – Distribution of flight distance of automobile, *L*.

the cylinder center, whose flight distance is *L*, can be conservatively calculated via Eq. (19).

$$q(\mathbf{r},L)=\begin{cases}0 & (\text{if } 0\le L\le r-R_t)\\ \frac{1}{\pi}\sin^{-1}\left(\frac{R_t}{r}\right) & (\text{if } r-R_t<L)\end{cases} \tag{19}$$

Then, the conditional strike probability under a specific local wind speed condition $Q_V(\mathbf{r})$ can be obtained by integration of the product of $S_V(L)$ and $q(\mathbf{r},L)$ over *L via* Eq. (16), as shown below.

$$Q_V(\mathbf{r})=\int_0^{\infty} q(\mathbf{r},L)S_V(L)dL=\frac{1}{\pi}\sin^{-1}\left(\frac{R_t}{r}\right)\int_{r-R_t}^{L_m} S_V(L)dL \tag{20}$$

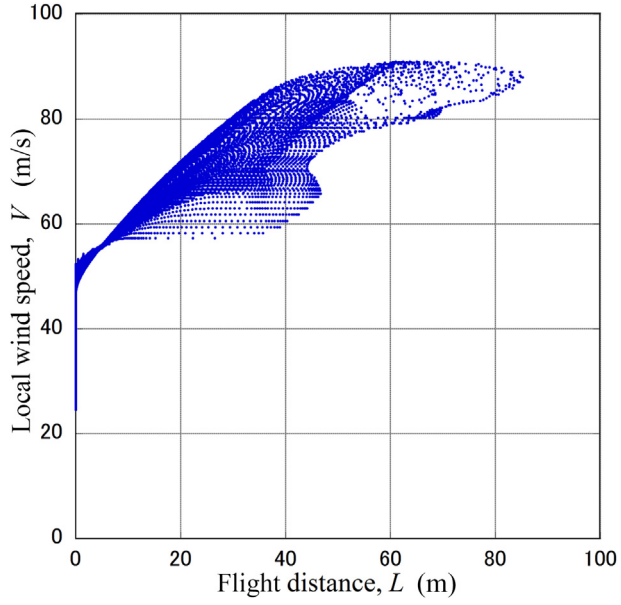

Fig. 10 – Phase plot of local wind speed, V, and flight distance, *L*.

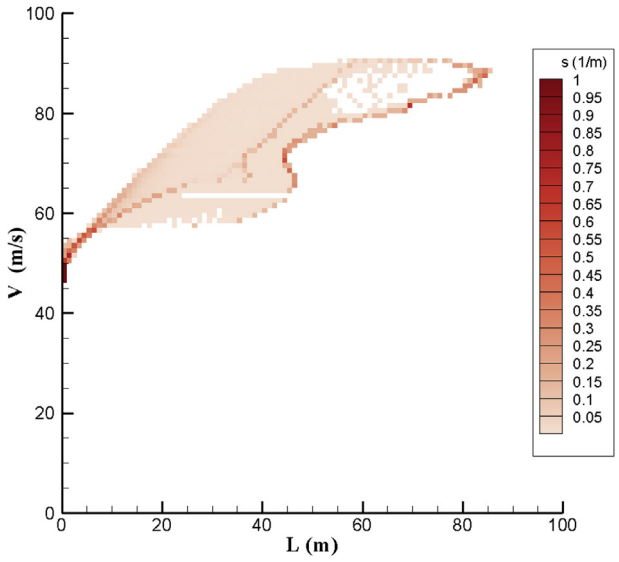

Fig. 11 – Example of the probability density function, $S_V(L)$.

In this numerical example, the annual exceedance probability of the local wind speed at a certain point, $H(V)$, is hypothetically assumed to be expressed by an exponential function, such that $H(V) = 10^{-6}$/y at V = 70 m/s and $H(V) = 10^{-7}$/y at V = 92 m/s, i.e., $H(V) = 0.00152\exp(-0.10466V)$. With these assumed data, the annual strike probability of the automobile on the structure, $P_h(\mathbf{r})$, is computed using Eq. (18), yielding the result shown in Fig. 13.

4. Discussion

4.1. *Qualitative and quantitative validation*

Fig. 10 indicates that the minimum local wind speed required for liftoff at 10 m AGL, V_c, is about 45 m/s. Because of the

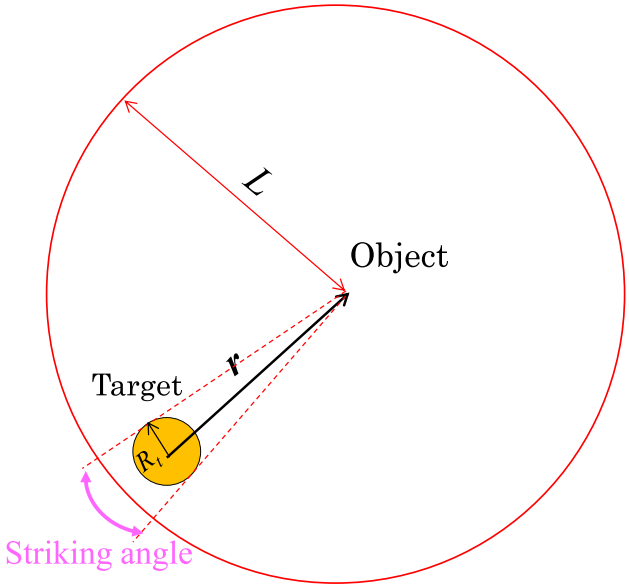

Fig. 12 – Geometrical condition of object and target.

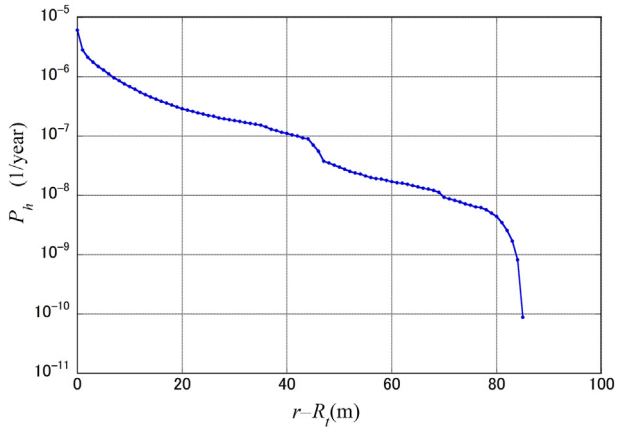

Fig. 13 – Annual strike probability of an automobile on the structure, P_h.

vertical profile of the wind speed, V_c should be slightly larger than the critical liftoff wind speed at the level of the automobile on the ground, U_c. We can confirm this relation with the value of 40.6 m/s estimated by $U_c = (mg/(0.5\rho C_D A))^{0.5}$, which is derived from the balance of the gravitational force and the lift force.

Besides this, we shall confirm not only the qualitative validity of the result, but also the quantitative consistency for two special cases in which the automobile is located in the vicinity of or far away from the structure. The annual exceedance probability of local wind speed, $H(V_c)$, at the minimum local wind speed, 45 m/s, is calculated as 1.37×10^{-5}/y via $H(V) = 0.00152 \exp(-0.10466V)$, which is the probability that the automobile will detach from the ground and fly for any distance and in any direction. If the automobile is located just in the vicinity of the structure, the possibility of a strike should be almost half of $H(V_c)$, owing to the requirement of $V > V_c$ and the uniform chance of the flight direction. Therefore, the probability of an automobile strike on the structure should be approximately half of 1.37×10^{-5}, i.e., 6.85×10^{-6}/y. The P_h value at $r = R_t$, shown in Fig. 13, is very close to this value, indicating the quantitative consistency of the result. Furthermore, the P_h value drastically decreases beyond $r = R_t + 80$, as can be seen in Fig. 13, which is consistent with the maximum flight distance of the automobile, i.e., about 83 m.

4.2. *Effect of tornado pressure distribution on flight behavior*

In this subsection, we discuss whether or not a pressure depression in the center of a tornado can affect the flight behavior. For simplicity, assuming the flow with the Rankine vortex model, the pressure distribution can be theoretically derived as shown below:

$$\frac{p}{\rho V_m^2} = \begin{cases} \frac{1}{2}\left(\frac{r}{R_m}\right)^2 - 1 & (r \le R_m) \\ -\frac{1}{2}\left(\frac{R_m}{r}\right)^2 & (r > R_m) \end{cases} \tag{21}$$

The aerodynamic force due to the pressure distribution acting on the object, $\mathbf{F}_B$, can be computed using the following integrals.

$$\mathbf{F}_B = -\int_S p\mathbf{n}dS = -\int_B \nabla p dB, \tag{22}$$

where S, B, and **n** are the surface of the object, the volume of the object, and a unit outward normal vector on the object surface, respectively. The pressure gradient can be calculated from Eq. (21) as follows for $x > 0$ and $y > 0$.

$$\nabla p = \left(\rho V_m^2 \min\left(\frac{x}{R_m^2}, \frac{R_m^2 x}{r^4}\right), \rho V_m^2 \min\left(\frac{y}{R_m^2}, \frac{R_m^2 y}{r^4}\right), 0\right) \tag{23}$$

With Eqs. (22) and (23), the magnitude of the force due to the pressure distribution, $|\mathbf{F}_B|$, can be approximately expressed in the following form:

$$|\mathbf{F}_B| = |\nabla p| B = \frac{\rho V_m^2 B}{R_m} \min\left(\frac{r}{R_m}, \frac{R_m^3}{r^3}\right) \tag{24}$$

By contrast, the magnitude of the aerodynamic force due to drag, $|\mathbf{F}_A|$, is approximately expressed by Eq. (25), assuming the stationary Rankine vortex as the tornado wind field for a stationary object.

$$|\mathbf{F}_A| = \frac{1}{2}\rho C_D A V_m^2 \min\left(\frac{r^2}{R_m^2}, \frac{R_m^2}{r^2}\right) \tag{25}$$

Then, the ratio of both the magnitudes, $|\mathbf{F}_B|/|\mathbf{F}_A|$, can be expressed as below.

$$\frac{|\mathbf{F}_B|}{|\mathbf{F}_A|} = \frac{2B}{C_D A r} \tag{26}$$

This ratio is much lower than unity in the outside region of the tornado core ($r > R_m$) and around the core radius ($r = R_m$), because $2B/C_D A$ is equivalent to the length scale of the object, and is much smaller than the tornado scale, R_m. By contrast, around the tornado center ($r << R_m$), $|\mathbf{F}_B|$ as well as $|\mathbf{F}_A|$ approaches zero as radius r decreases, suggesting that the gravitational force prevails. The above discussion suggests that tornado pressure distribution will not significantly affect the flight behavior.

In the case of the Fujita model, Eguchi et al [18] computed the pressure distribution by solving a pressure Poisson equation with an appropriate boundary condition, and demonstrated that the pressure depression of the Fujita model is weaker than that of the Rankine vortex model. This implies the same conclusion for the wind field of the Fujita model, as shown above.

5. Conclusion

The authors have formulated an efficient method to evaluate the probability of tornado missile strike without using the Monte Carlo method. Using a computational code, TONBOS, a stochastic correlation between the local wind speed, V, and the flight distance, L, was computed for a large number of objects initially placed around a tornado path; the correlation was used to evaluate the conditional strike probability. By

contrast, annual exceedance probability of local wind speed, derivable using a tornado hazard analysis code, was utilized to obtain the probability density function of the local wind speed; then, the annual probability of tornado missile strike on a structure was computed by combining the conditional strike probability and the probability density function of the local wind speed. The evaluation method was applied to the evaluation of strike probability of an automobile on a tall cylindrical structure. The results demonstrated qualitative validity and quantitative consistency for special cases in which an object is located just near or away from the structure.

In the numerical examples presented in this paper, tornado intensity and radius were specific values. To obtain missile strike probability and its uncertainty in the true sense of probabilistic assessment, variations of tornado characteristics such as intensity and scale have to be incorporated into the strike probability evaluation. Furthermore, temporal variations of the aerodynamic force during missile flight may need to be taken into account. We believe that the method presented here can be improved in such directions as our future work.

Conflicts of interest

All the authors have no conflicts of interest to declare.

Acknowledgments

The authors gratefully acknowledge the fruitful comments from Mr Masashi Kuramasu (The Chugoku Electric Power Co., Inc.) and from Dr Keisuke Nakao (Central Research Institute of Electric Power Industry) in developing the evaluation method proposed in the paper.

REFERENCES

[1] L.A. Twisdale, W.L. Dunn, T.L. Davis, Tornado missile transport analysis, Nucl. Eng. Des. 51 (1979) 295–308.
[2] EPRI, Tornado Missile Simulation and Design Methodology, Volume 1: Simulation Methodology, Design Applications, and TORMIS Computer Code, NP-2005–V1, 1981.
[3] EPRI, Tornado Missile Simulation and Design Methodology, Volume 2: Model Verification and Database Updates, NP-2005–V2, 1981.
[4] K.D. Hope, N. Povroznyk, R. Schneider, Tornado Missile Strike Calculator: an Excel-based stochastic model of tornado-driven missile behavior for use in high winds PRA, International Topical Meeting on Probabilistic Safety Assessment and Analysis (PSA 2015), Sun Valley, Idaho, USA, 2015, p. 12086.
[5] Y. Eguchi, S. Sugimoto, Y. Hattori, H. Hirakuchi, Development of TONBOS for simulation of liftoff and flight of objects driven by a tornado, Central Research Institute of Electric Power Industry, Civil Engineering Research Laboratory Report, No. N14002, 2014 (in Japanese).
[6] Y. Eguchi, S. Sugimoto, Y. Hattori, H. Hirakuchi, A rational method to evaluate tornado-borne missile speed in nuclear power plants (validation of a numerical code based on Fujita's tornado model), Trans. JSME 81 (2015) 823 (in Japanese).
[7] Y. Eguchi, T. Murakami, M. Kuramasu, H. Hirakuchi, S. Sugimoto, Y. Hattori, Annual probability of tornado missile strike on structure using Fujita model, 2016 Spring Meeting of the Atomic Energy Society of Japan, 2016, p. 2P10 (in Japanese).
[8] H. Hirakuchi, D. Nohara, S. Sugimoto, Y. Eguchi, Tornado wind hazard evaluation method for nuclear power plants, Proc. Annual Meeting 2015, Japan Association for Wind Engineering, 2015, pp. 133–134 (in Japanese).
[9] T.T. Fujita, Workbook of Tornadoes and High Winds for Engineering Applications, University of Chicago, 1978.
[10] E. Simiu, M. Cordes, Tornado-Borne Missile Speeds, NBSIR 76–1050, 1976.
[11] E. Simiu, R.H. Scanlan, Wind Effects on Structures: Fundamentals and Applications to Design, third ed., John Wiley & Sons, Hoboken, NJ, 1996.
[12] EPRI, Wind Field and Trajectory Models for Tornado Propelled Objects, NP-748, 1978.
[13] K. Hayashi, K. Ooi, M. Maeda, R. Saitou, Fluid forces acting on a cube and a strip roughness submerged in open channel flow, J. Jpn. Soc. Civil Eng. B1 (Hydraul. Eng.) 67 (2011) I_1141–I_1146 (in Japanese).
[14] H. Matsumiya, K. Nakaoka, T. Nishihara, K. Kimura, Wind tunnel test for the ground effect of aerodynamic force on a photovoltaic panel, J. Struct. Eng. A 60 (2014) 446–454 (in Japanese).
[15] K. Yamamoto, K. Hayasi, M. Senkine, K. Fujita, M. Tamura, S. Nisimura, K. Hamaguchi, Measuring method of drag coefficient, lift coefficient and equivalent roughness of revetment block, Annu. J. Hydraul. Eng. 44 (2000) 1053–1058 (in Japanese).
[16] T. Schmidlin, B. Hammer, P. King, Y. Ono, L.S. Miller, G. Thumann, Unsafe at any (wind) speed? Testing the stability of motor vehicles in severe winds, Bull. Am. Meteorol. Soc. 83 (2002) 1821–1830.
[17] M.R. Ahmed, S.D. Sharma, An investigation on the aerodynamics of a symmetrical airfoil in ground effect, Exp. Thermal Fluid Sci. 29 (2005) 633–647.
[18] Y. Eguchi, S. Sugimoto, H. Hattori, H. Hirakuchi, Tornado pressure retrieval from Fujita's engineering model DBT-77, Proceedings of the 6th Int. Conf. on Vortex Flows and Vortex Models, 2014, Nagoya, Japan.